ON BAROTROPIC AND BAROCLINIC MODELS, WITH SPECIAL EMPHASIS ON ULTRA-LONG WAVES

A. WIIN-NIELSEN, Air Weather Service
Joint Numerical Weather Prediction Unit, Suitland, Md.

[Manuscript received April 1, 1959; revised May 22, 1959]

ABSTRACT

The problem of control of the ultra-long waves in numerical prediction is considered. Sections 2–4 contain a discussion of the one-level forecasts. It is shown that the vertical variation of the horizontal wind and the static stability are the main factors in determining the value of divergence at 500 mb. An independent estimate of the size of the term governing the ultra-long waves in the atmosphere agrees well with the one determined by Cressman on an empirical basis.

Section 5 points out that any two-parameter model has to contain an effect similar to the one contained in the one-parameter model controlling the ultra-long waves. A modification of a two-parameter model is made in such a way that the ultra-long waves are controlled.

Section 6 describes a perturbation analysis of the model developed in Section 5 in order to investigate the effect of the modification also on the shorter waves. It is found that a certain stabilization of the shorter waves is produced. Baroclinic instability and growth rate are investigated.

Sections 7 and 8 contain a justification of certain approximations used in the earlier sections regarding the vertical variation of static stability and the profile of vertical velocity.

1. INTRODUCTION

The Joint Numerical Weather Prediction Unit has recently improved the 500-mb. barotropic forecasts by paying special attention to the behavior of the very long atmospheric waves. The non-divergent barotropic forecasts were first empirically corrected by Wolff [18], who used the observed fact that the very long atmospheric waves do not change either position or ampltitude to any great extent from day to day. He therefore forced the waves with wave-number one, two, and three to be stationary throughout the forecast period. Shortly after, Cressman [6] used a special case of Phillips' [13] two-layer model to show that a model atmosphere consisting of two homogeneous layers, where the motion in the lower fluid is parallel to the contour of the interface, and where the motion in the upper fluid is negligible, would decrease the retrogression of the very long atmospheric waves to a considerable extent. The forecast equation used by Cressman is the same as the one used by Bolin [2] in his so-called tropopause model. Both of these authors had difficulties in the determination of the proper value for certain constants appearing in the prognostic equation, mainly because a model atmosphere consisting of two homogeneous layers is rather difficult to "translate" to the real atmosphere. Cressman decided therefore to determine the value of the coefficient by computing a number of forecasts on the same data with different values of the coefficient and then choosing the coefficient that gave the best forecast. This procedure may not lead to the proper value of the coefficient, because a minimization of forecast height errors with respect to the coefficient might tend to compensate for correlated, but physically unrelated errors, as was also mentioned by Cressman.

In view of the situation mentioned above it seems to be in order to try to formulate the barotropic, divergent model in such a way that the value of the constants can more easily be related to the real atmosphere. Sections 2 through 4 of this paper are devoted to this purpose.

An analysis of baroclinic instability and especially of the phase-speed of waves in a baroclinic atmosphere, as for instance made by Eliassen [9], shows that the phase-speed for large values of the wavelength approaches the Rossby speed for a non-divergent atmosphere. For large values of the wavelength one actually obtains two solutions for the phase-speed. One of them is not likely to be observed in the atmosphere because it corresponds to a situation where the temperature wave is out of phase with the pressure, corresponding to warm troughs and cold ridges. The other solution is the one approaching the Rossby speed.

This result shows that one will find about the same difficulties as in the non-divergent barotropic model with respect to the ultra-long waves, when one integrates a baroclinic model of the usual type over an almost hemispheric region. It is therefore a necessity to correct the baroclinic forecast equations in such a way that the

511937—59——2

retrogression of the ultra-long waves is reduced to a considerable extent. Section 5 describes a simple two-parameter model where this effect is included.

Recently Burger [3] pointed out that the vorticity equation loses its prognostic value when the wavelength is of the same order of magnitude as the radius of the earth. As long as we base our forecasts on the vorticity equation we can therefore probably not do anything better than express the quasi-stationary character of the ultra-long waves. The two models presented here do therefore not claim to have any skill in the regime of the ultra-long waves. The problem which has been attacked is to incorporate effects in barotropic and baroclinic models which control the long waves and at the same time to investigate the changes which may be caused by such effects on the shorter waves.

2. DERIVATION OF THE PROGNOSTIC EQUATION IN THE BAROTROPIC CASE

In the derivation we shall consider the vorticity equation in the form

$$\frac{\partial \zeta}{\partial t}+\mathbf{V}\cdot\nabla\eta=f_0\frac{\partial \omega}{\partial p} \tag{2.1}$$

where $\mathbf{V}$ is the horizontal wind vector, ζ is the vertical component of the relative vorticity, $\eta=\zeta+f$, f is the Coriolis parameter, and $\omega=dp/dt$ the vertical velocity in a coordinate system with pressure as the vertical coordinate.

This form of the vorticity equation, where the value of the Coriolis parameter in the divergence term is a standard value, $f=f_0$, is consistent with certain general integral constraints, as shown by the author [17], when the horizontal wind in the vorticity advection term is nondivergent. The derivation of the barotropic vorticity equation is usually based upon the equivalent-barotropic atmosphere (Charney [5]), where the horizontal wind in the complete atmosphere is assumed to vary vertically in strength, but not in direction. It is then shown that the simple barotropic vorticity equation can be applied to the vertical mean flow in the atmosphere provided the effect of surface pressure changes is neglected. The assumption

$$\mathbf{V}=A(p)\mathbf{V}^* \tag{2.2}$$

which defines the equivalent-barotropic atmosphere and where $\mathbf{V}^*$ for instance may be taken as the 500-mb. flow, will in general apply with good accuracy in a layer around the 500-mb. level, while the accuracy becomes smaller the farther we are from the 500-mb. level. We shall in the following make use of (2.2) only in a thin layer around the 500-mb. level. Equation (2.2) expresses then, according to the geostrophic thermal wind relation, that the thermal wind is parallel to the wind itself, or in other words that the isotherms at 500 mb. are parallel to the contour lines. The last requirement is probably fulfilled to the greatest extent in the mid-troposphere, while temperature advection by the horizontal wind is greater both higher up and lower down in the troposphere, according to observations.

The equivalent-barotropic atmosphere is usually treated without any reference to the thermodynamics of the atmosphere. If, however, the relation (2.2) is approximately satisfied at least around the 500-mb. level it must mean that the local temperature changes to the largest extent are compensated by vertical velocities, and that the adiabatic equation therefore takes the form

$$\frac{\partial}{\partial t}\left(\frac{\partial \phi}{\partial p}\right)+\sigma\omega=0, \quad \sigma=-\alpha\frac{\partial \ln\theta}{\partial p} \tag{2.3}$$

at the 500-mb. level. In (2.3) $\phi=gz$ is the geopotential, α the specific volume, and θ the potential temperature.

The expression (2.2) applies actually to the distribution of the horizontal wind. If the horizontal wind is assumed quasi-geostrophic, we obtain from (2.2):

$$\frac{\partial}{\partial t}\left(\frac{\partial \phi}{\partial p}\right)=\frac{dA}{dp}\frac{\partial \phi^*}{\partial t}. \tag{2.4}$$

The vertical velocity can then be obtained from (2.3) in the form:

$$\omega=-\frac{dA/dp}{\sigma}\frac{\partial \phi^*}{\partial t}. \tag{2.5}$$

We shall further in the thermodynamic equation (2.5) replace the geopotential ϕ^* by a stream function ψ^* satisfying the relation

$$\psi^*=\frac{\phi^*}{f_0}. \tag{2.6}$$

The implication of this assumption in the thermodynamic equation, and only here, has been discussed by Phillips [15]. Introducing (2.6) in (2.5) we obtain:

$$\omega=-\frac{dA/dp}{\sigma}f_0\frac{\partial \psi^*}{\partial t}. \tag{2.7}$$

In order to obtain the prognostic equation from (2.1) it is now necessary to evaluate $\partial\omega/\partial p$ from (2.7). Let us assume for simplicity that dA/dp is a constant. The main problem is then in which way the vertical stability σ varies with pressure. It will be shown (section 7) that a variation of the vertical stability expressed by the formula

$$\sigma=\sigma^*\left(\frac{p}{P}\right)^{-2}, \quad P=500 \text{ mb.} \tag{2.8}$$

describes the vertical variation of temperature in a mean atmosphere with good accuracy. In (2.8) σ^* is the static stability at 500 mb. The accuracy is especially good around 500 mb., because the vertical stability at 500 mb. is used to fit the distribution (2.8) to the atmosphere.

From (2.7) and (2.8) we obtain then, provided $A(p)$ varies linearly with pressure:

$$\left(\frac{\partial\omega}{\partial p}\right)_{500}=-\frac{2f_0}{\sigma^*P}\left(\frac{dA}{dp}\right)\frac{\partial\psi^*}{\partial t} \tag{2.9}$$

which, inserted in (2.1), leads to the prognostic equation:

$$\frac{\partial}{\partial t}(\nabla^2\psi^*-q\psi^*)+J(\psi^*,\eta^*)=0 \tag{2.10}$$

where

$$q=\frac{2f_0^2}{\sigma^*P}\cdot\left(-\frac{dA}{dp}\right). \tag{2.11}$$

3. DISCUSSION OF THE PROGNOSTIC EQUATION

The Helmholz term appearing in (2.10) is in this formulation due to two factors, the increase of the horizontal wind with height and the decrease of temperature with height in the atmosphere. Both of these factors are well known from observations, and it is therefore somewhat easier to determine the proper value of q to be used here than in Bolin's and Cressman's prognostic equations. In order to determine q we need a value for σ^* and for $(-dA/dp)$.

The value for σ^* may be determined from the expression

$$\sigma=-\alpha\frac{\partial\ln\theta}{\partial p}=\frac{R^2T}{gp^2}(\gamma_d-\gamma) \tag{3.1}$$

where R is the gas constant, γ_d the dry adiabatic lapse rate, and γ the local lapse rate.

It has been the general experience among people working with models in numerical prediction that the standard atmosphere is too unstable. Using $\gamma=0.5°$ C. per 100 m., which corresponds to about 80 percent of γ in the standard atmosphere, we obtain:

$$\sigma^*=4.2 \text{ MTS units.} \tag{3.2}$$

We have already assumed that $A(p)$ varies linearly with pressure in the derivation of (2.9). We may now obtain dA/dp by noting that $A(p^*)=1$ according to (2.2) and further assume that $A(2P)=0.2$, which means that the surface wind is about 20 percent of the 500-mb. wind, an assumption used, for instance, in the incorporation of the mountain effect in the barotropic model. This gives:

$$-dA/dp=0.8/P=16\times10^{-3} \tag{3.3}$$

and

$$q\cong1.5\times10^{-12} \tag{3.4}$$

The prognostic equation (2.10) may now be compared with Cressman's prognostic equation reproduced here without the term accounting for the mountain effect:

$$\frac{\partial}{\partial t}\left(\nabla^2\psi^*-\mu\frac{\eta^*}{\overline{\psi^*}}\psi^*\right)+J(\psi^*,\eta^*)=0 \tag{3.5}$$

In this equation the symbols have the same meaning as before. $\overline{\psi^*}$ is a representative mean value of the stream function obtained through the solution of the balance equation, while μ is the coefficient, which actually is equal to $1\Big/\frac{h}{z}\left(1-\frac{\rho'}{\rho}\right)$ where h is the height of the interface, z the height of the 500-mb. surface, and ρ' and ρ the densities of the upper and lower fluid. We are now in the position to evaluate the value of μ, which would correspond to the estimate of q given in (3.4), if we linearize the coefficient in (3.5). We obtain then:

$$\mu=\frac{g\overline{z^*}}{f_0^2}\,q\simeq8 \tag{3.6}$$

This independent estimate of μ is about equal to the highest value of μ used by Cressman in his empirical determination of the coefficient. Cressman varied μ from 0 to 8. It will be seen that μ is inversely proportional to σ^*. A value of σ^* higher than the one used here corresponding to $\gamma=0.5°$C./100 m. is probably not possible as a mean value for the atmosphere. If we therefore accept this value of σ^*, it is found that values of μ less than 8 can be obtained only with $-dA/dp$ smaller than the value used here. It is interesting to note that a value of $\mu=4$, which is the value used at the moment in the operational forecasting, would correspond to $-dA/dp=0.4/P$. This would mean that the surface wind should be about 60 percent of the 500-mb. wind, which sounds unreasonable. On the basis of this discussion one is therefore tempted to conclude that a value of μ somewhat greater than 4 ought to be used.

4. A SIMPLE WAVE ANALYSIS

It is of interest to make a simple wave analysis of the prognostic equation (2.10) in order to obtain a first idea of the influence which different values of q will have on the motion of long and short waves in the atmosphere.

Consider a stream function

$$\psi(x,y,t)=-Uy+Ae^{ik(x-ct)} \tag{4.1}$$

where the superscript * now has been dropped and where $U=$constant is the zonal component of the wind. This stream function will satisfy (2.10) provided the phase speed c satisfies the relation

$$c=\frac{U-\beta/k^2}{1+q/k^2}=\frac{c_{ND}}{1+q/k^2} \tag{4.2}$$

In the derivation of (4.2) $\beta=df/dy$ has been considered as constant and is evaluated at 45° N. $k=2\pi/L$, where L is the wavelength. If N is the number of waves around the hemisphere, i.e., $2\pi R\cos\varphi=N\cdot L$, we may also write (4.2) in the form

$$c=\frac{U-2\Omega R\cos^3\varphi/N^2}{1+qR^2\cos\varphi/N^2} \tag{4.3}$$

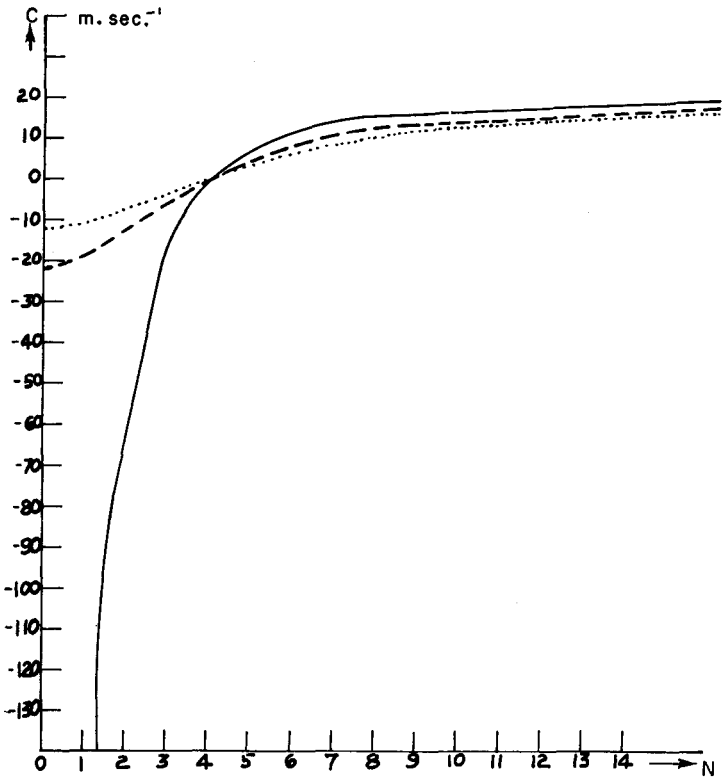

FIGURE 1.—Phase velocity as a function of number of waves around the hemisphere. The solid line corresponds to $q=0$, the dashed line to $q=(3/4)10^{-12}$ and the dotted line to $q=(3/2)10^{-12}$.

The values of c shown in figure 1 in m. sec.$^{-1}$ are computed for $U=20$ m. sec.$^{-1}$, $\varphi=45°$ N., and for $q=0$, $(3/4)\times10^{-12}$, and $(3/2)\times10^{-12}$, which would correspond to approximately $\mu=0$, 4, and 8. It is seen that $q=(3/2)\times10^{-12}$, the value estimated in this study, reduces the retrogression further than the operational value. For wave number 1 the phase-velocity changes from about -19 m. sec.$^{-1}$ to about -11 m. sec.$^{-1}$, while on the other hand c is changed from 12 m. sec.$^{-1}$ to 10 m. sec.$^{-1}$ for $N=8$, corresponding to a wavelength of about 3500 km. It is therefore likely that a change of q from the present value, $(3/4)\times10^{-12}$, to the value determined here, $(3/2)\times10^{-12}$, would not change the forecast appreciably, except for the ultra-long waves, which in fact are better forecasted by the greater value of q, according to Cressman.

5. THE BAROCLINIC CASE

The incorporation of a control of the ultra-long waves in a baroclinic model is complicated by the fact that we want the corrected model to keep essentially the same properties it had for the shorter waves. A pronounced difference between a barotropic and a baroclinic model is that the baroclinic model contains a mechanism for instability by which waves may grow in amplitude. Once we have decided in which way we want to incorporate the control of the long waves we have therefore to investigate whether the phase-speed and the instability criteria for the modified model are left essentially unchanged, or if they are changed, we have to investigate whether the change is in a direction which is supported by observations or experience.

One of the results in the first sections of this paper is that the behavior of the ultra-long waves is sensitive to even very small divergences. We may therefore expect that if we introduce a mean divergence different from zero in a baroclinic model we will be able to control the ultra-long waves. The main problem is to relate the mean divergence to the parameters which carry the history of the flow. It means, for a two-parameter model of the usual type, to a height and a thickness. In the following simple two-parameter model we shall try to introduce such a net divergence in the vertical direction by relating the vertical mean divergence to the flow parameters in a way similar to the one used in the barotropic case treated earlier in this paper.

The prognostic equations we are going to use will be the vorticity equation in the form:

$$\frac{\partial\zeta}{\partial t}+\mathbf{V}\cdot\nabla(\zeta+f)=f_0\frac{\partial\omega}{\partial p} \tag{5.1}$$

and the adiabatic equation

$$\frac{\partial}{\partial t}\left(\frac{\partial\psi}{\partial p}\right)+\mathbf{V}\cdot\nabla\left(\frac{\partial\psi}{\partial p}\right)+\frac{\sigma}{f_0}\omega=0 \tag{5.2}$$

where f_0 is a standard value of the Coriolis parameter.

We shall in the following denote the 200, 400, 600, 800, and 1000-mb. surfaces with subscripts 0, 1, 2, 3, and 4. Applying equation (5.1) to the 400 and 800-mb. surfaces and approximating $\partial\omega/\partial p$ by finite differences we obtain with $P=40$ cb.:

$$\frac{\partial\zeta_1}{\partial t}+\mathbf{V}_1\cdot\nabla(\zeta_1+f)=\frac{f_0}{P}(\omega_2-\omega_0) \tag{5.3}$$

and

$$\frac{\partial\zeta_3}{\partial t}+\mathbf{V}_3\cdot\nabla(\zeta_3+f)=\frac{f_0}{P}(\omega_4-\omega_2). \tag{5.4}$$

We shall in the following apply the approximate boundary condition $\omega_4=0$, thereby disregarding mountain effects in the model. The practice before has been to set $\omega_0=0$. This means that we assume that the vertical velocity has a zero point somewhere between the two zero points at the surface of the earth and at the top of the atmosphere. Although it is true that such a zero point exists in most cases the result is that putting this zero point invariably at 200 mb. reduces the vertical mean divergence in the layer between 200 and 1000 mb. to zero, and we cannot any longer control the long waves. We shall therefore not put $\omega_0=0$, but try to work with the layer between 1000 mb. and 200 mb. as an "open" system.

With $\omega_4=0$ it is now convenient to add and subtract the equations (5.3) and (5.4). At the same time we shall

assume that for any quantity α we have

$$\alpha_2=\frac{1}{2}(\alpha_1+\alpha_3) \tag{5.5}$$

and we shall further introduce the notation:

$$\alpha'=\frac{1}{2}(\alpha_1-\alpha_3). \tag{5.6}$$

Using this procedure we obtain:

$$\frac{\partial\zeta_2}{\partial t}+\mathbf{V}_2\cdot\nabla(\zeta_2+f)+\mathbf{V}'\cdot\nabla\zeta'=-\frac{f_0}{2P}\omega_0 \tag{5.7}$$

$$\frac{\partial\zeta'}{\partial t}+\mathbf{V}_2\cdot\nabla\zeta'+\mathbf{V}'\cdot\nabla(\zeta_2+f)=\frac{f_0}{P}\omega_2-\frac{f_0}{2P}\omega_0. \tag{5.8}$$

By applying the adiabatic equation at 600 mb. the value for ω_2 may now be obtained in the usual way:

$$\frac{f_0}{P}\omega_2=\frac{2f_0^2}{\sigma_2P^2}\left(\frac{\partial\psi'}{\partial t}+\mathbf{V}^*\cdot\nabla\psi'\right)=q\left(\frac{\partial\psi'}{\partial t}+\mathbf{V}^*\cdot\nabla\psi'\right) \tag{5.9}$$

with

$$q=\frac{2f_0^2}{\sigma_2P^2}\simeq\text{constant}. \tag{5.10}$$

The value of $\omega_0/2P$ may be related to the parameters characterizing the flow in the following way. Let us apply the continuity equation at 400 and 800 mb. and obtain

$$\nabla\cdot\mathbf{V}_1=-(\partial\omega/\partial p)_1=-\frac{\omega_2-\omega_0}{P} \tag{5.11}$$

$$\nabla\cdot\mathbf{V}_3=-(\partial\omega/\partial p)_3=\frac{\omega_2}{P}. \tag{5.12}$$

Adding these two equations we obtain:

$$\nabla\cdot\mathbf{V}_2=\frac{\omega_0}{2P}. \tag{5.13}$$

We have on the other hand:

$$\overline{\nabla\cdot\mathbf{V}}=\frac{1}{2P}\int_{P/_2}^{5P/_2}\nabla\cdot\mathbf{V}\,dp=\frac{\omega_0}{2P} \tag{5.14}$$

where $\overline{\nabla\cdot\mathbf{V}}$ is the vertically averaged divergence in the layer between 200 and 1000 mb. According to (5.13) and (5.14) $\nabla\cdot\mathbf{V}_2$ represents within the approximations of the model the vertically averaged divergence. Due to the relation (5.13) we are in the position to express $\omega_0/2P$ by a procedure similar to the one used in the barotropic case.

In the incorporation of the mean divergence in the two-parameter model we should have in mind that we are first of all trying to control the behavior of the ultra-long waves. In the first approximation we are probably therefore allowed to express $\overline{\nabla\cdot\mathbf{V}}$ in the same way as in the barotropic case i.e.,

$$-\frac{f_0}{2P}\omega_0=-f_0\nabla\cdot\mathbf{V}_2=r\frac{\partial\psi_2}{\partial t} \tag{5.15}$$

with

$$r=\frac{f_0^2}{\sigma_2^2}\left(\frac{d\sigma}{dp}\right)_2\frac{dA}{dp}. \tag{5.16}$$

With $f_0=10^{-4}$ sec.$^{-1}$, $\sigma_2=3$ MTS units, $dA/dp=-\frac{0.8}{P}$, and $(d\sigma/dp)_2$ computed from a formula corresponding to (2.8) we arrive at a value of

$$r=2.22\times10^{-12}. \tag{5.17}$$

The assumption (5.15) means that we assume the ultra-long waves to have a small tilt vertically around level 2; i.e. 600 mb. It is realized that this assumption needs further investigation. In a paper by Eliasen [10] it is shown that the tilt of the long waves on the seasonal mean charts is not insignificant in the lower part of the troposphere. On the other hand, a similar Fourier analysis of the long waves at the levels 800, 700, 500, 300, and 200 mb. on a few individual days has in no case shown tilts nearly as great as those found on the normal charts. The assumption (5.15) may therefore in many cases be considered as a good first approximation.

The expression (5.15) could be introduced directly in (5.7) and (5.8). However, diagnostic computations of the vertical profile of the vertical velocity described in section 8, show that $\omega_0\ll\omega_2$. For simplicity we shall therefore neglect the second term on the right side of (5.8) in comparison with the first. This means only that we are neglecting the mean divergence in the troposphere in comparison with the divergence at 400 or 800 mb., which represent the upper and lower parts of the troposphere.

Granted that these approximations can be made we arrive at the following modified forecast equations

$$\frac{\partial\zeta_2}{\partial t}+\mathbf{V}_2\cdot\nabla(\zeta_2+f)+\mathbf{V}'\cdot\nabla\zeta'=r\frac{\partial\psi_2}{\partial t} \tag{5.18}$$

$$\frac{\partial\zeta'}{\partial t}+\mathbf{V}_2\cdot\nabla\zeta'+\mathbf{V}'\cdot\nabla(\zeta_2+f)=q\left(\frac{\partial\psi'}{\partial t}+\mathbf{V}_2\cdot\nabla\psi'\right). \tag{5.19}$$

The only change which in fact has been made is that the term $r\frac{\partial\psi_2}{\partial t}$ has been added to the first prognostic equation, when we compare with the equations for a model where the mean divergence is zero.

It is the purpose of the following section to show that this small modification will control the ultra-long waves in the atmosphere and further to illustrate the changes which we may expect in the short waves using (5.18) and (5.19) as prognostic equations.

6. A PERTURBATION ANALYSIS OF THE BAROCLINIC CASE

Although the final proof of the applicability of a set of prognostic equations always is the successful forecasts

made from them it is of interest to make a simple analysis of the model in order to test it as far as the mathematical technique allows us to do it. The only test which can be made by a relatively simple mathematical technique is a linear perturbation investigation. The two-parameter models where the mean divergence vanishes have been investigated in this way by, for instance, Eliassen [9], Thompson [16], and Phillips [14]. It is therefore of considerable interest to make a comparative study of the model described here and the corresponding model with vanishing mean divergence.

The two parameters that characterize the model are the stream functions ψ_2 and ψ'. Let these be described by the relations

$$\psi_2(x,y,t)=-U_2y+\hat{\psi}_2e^{ik(x-ct)} \tag{6.1}$$

and

$$\psi'(x,y,t)=-U'y+\hat{\psi}'e^{ik(x-ct)} \tag{6.2}$$

where U_2 and U' are constants, $\hat{\psi}_2$ and $\hat{\psi}'$ are the amplitudes, $k=2\pi/L$ is the wave number, and c is the phase-speed (wave velocity).

Inserting (6.1) and (6.2) into (5.18) and (5.19) one finds that ψ_2 and ψ' are solutions to the prognostic equations provided

$$c=\frac{2+r^*}{2(1+r^*)}U_2-\frac{2+r^*+q^*}{2(1+r^*)(1+q^*)}\beta^*\pm\frac{\sqrt{D}}{2(1+r^*)(1+q^*)}. \tag{6.3}$$

For any quantity α the superscript * means

$$\alpha^*=\frac{\alpha}{k^2} \tag{6.4}$$

Further

$$D=[(1+q^*)\,r^*\,U_2+(q^*-r^*)\,\beta^*]^2-4\,(1+r^*)(q^{*2}-1)U'^2. \tag{6.5}$$

It should be mentioned that the corresponding formula for the usual two-parameter model with vanishing mean divergence simply may be obtained by putting $r^*\equiv 0$. This simple relation makes a comparison between the two models fairly easy.

As we are here especially interested in the ultra-long waves we shall first investigate what happens when $k\to 0$ ($L\to\infty$). Considering the three terms in (6.3) we find directly that

$$\left.\begin{aligned}&\lim_{k\to 0}\frac{2+r^*}{2(1+r^*)}U_2=\frac{1}{2}U_2\\&\lim_{k\to 0}\frac{2+r^*+q^*}{2(1+r^*)(1+q^*)}\beta^*=\frac{r+q}{2rq}\beta\\&\lim_{k\to 0}\frac{\sqrt{D}}{2(1+r^*)(1+q^*)}=\frac{1}{2}U_2+\frac{q-r}{2rq}\beta.\end{aligned}\right\} \tag{6.6}$$

We find therefore that

$$\lim_{k\to 0}c=\begin{cases}U_2-\dfrac{\beta}{q}, & \text{if the plus sign is chosen}\\[2ex] -\dfrac{\beta}{r}, & \text{if the minus sign is chosen}\end{cases} \tag{6.7}$$

The result (6.7) shows that both of these solutions remain finite for $k\to 0$. The interesting solution is the one corresponding to the minus sign. With the numerical values chosen here we find for the latter solution

$$c_{k=0}=-\beta/r=-7.2\ \text{m.sec.}^{-1} \tag{6.8}$$

as compared to $c_{k=0}=-\infty$ for $r=0$ corresponding to a vanishing mean divergence. We may therefore conclude that the model controls the ultra-long waves in the sense that the retrogression is greatly reduced.

Next, we shall investigate in which way the baroclinic instability is being changed by the introduction of a mean divergence. Unstable solutions are found in cases where

$$D<0 \tag{6.9}$$

From the expression (6.5) for D it is seen that only *stable* solutions are possible, when

$$q^*<1$$

With

$$q=\frac{2f_0^2}{\sigma_2P^2}\simeq 4\times 10^{-12}$$

we find that $q^*<1$, if $L<3.1\times 10^3$ km. Consequently all waves with a wavelength smaller than 3100 km. are stable. This result is the same as for the model with vanishing mean divergence.

Unstable solutions are possible if L is greater than this critical wavelength. The division between the unstable and stable region may be found by equating D to zero. It is seen immediately that a certain difference now appears between the models with and without mean divergence. In the case of no mean divergence the division between the stable and unstable region is given by a single relation between the models with and without mean divergence. However, when we have a mean divergence the zonal wind U_2 also enters into the relation. By inspection of (6.5) it is seen that the greater the velocity U_2 is, the greater U' has to be in order to create instability. This relation is illustrated in figure 2, where the critical vertical wind shear $(dU/dz)_c$ expressed now in the unit m. sec.$^{-1}$ km.$^{-1}$ is plotted as a function of wavelength in units of thousands of km. It is seen that the curve for $U_2=20$ m. sec.$^{-1}$ lies higher than the one corresponding to $U_2=10$ m. sec.$^{-1}$. The curve corresponding to no zonal velocity, $U_2=0$ m. sec.$^{-1}$, is also drawn as representing an extreme case. The dashed curve in figure 2 represents $(dU/dz)_c$ as a function of wavelength for the model with vanishing mean divergence. This curve is obtained from (6.5) by putting $r=0$.

Considering first the ultra-long waves we find that they are closer to an unstable situation in the model with mean divergence. However, disregarding the case where $U_2=0$ as an extreme case, we find that vertical wind shears as observed in the atmosphere would never make these waves unstable. We may therefore conclude that we have obtained a considerably reduced retrogression of ultra-long waves without introducing any instability in this part of the spectrum.

Turning our attention toward the smaller wavelength in the spectrum we find that the introduction of a mean divergence in the model changes the instability to some extent. We find for instance with the value of the static stability chosen here that the wavelength of maximum instability is around 4000 km. in both models. However, in the model without mean divergence a vertical shear of only 1.6 m. sec.$^{-1}$ km.$^{-1}$ is necessary to produce instability. The corresponding figures are about 3.1 and 5.8 m. sec.$^{-1}$ km.$^{-1}$ for U_2 equal to 10 m. sec.$^{-1}$ and 20 m. sec.$^{-1}$, respectively. Briefly, we may therefore conclude that the way in which we have introduced the mean divergence into the model tends to stabilize the shorter waves somewhat.

It is a general impression that a two-parameter model without mean divergence will develop pressure systems too much in cases when they actually are deepening. From the result of the instability analysis made here it is seen that a model with mean divergence will counteract this tendency. Actual computations will of course have to prove this tentative conclusion.

It has been pointed out by other investigators (Eady [8], Charney [4]) that according to linear baroclinic instability theory the westerlies should constantly be in a state of instability. The result that the present model seems to decrease the instability makes it interesting to investigate whether this also is the case for this model. Although our instability criterion is derived for flow patterns without horizontal shear we shall nevertheless try to compare the results with the mean state of the real atmosphere. The wavelength of maximum instability seems to be around 4000 km. We shall therefore investigate the problem mentioned above by setting $L=4000$ km. and then computing the critical vertical wind shear as a function of latitude using values of U_2; i.e., U at 600 mb., taken from a mean cross-section of the atmosphere. The critical wind shear may then be compared with the actual wind shear in the mean cross-section. For this purpose the mean cross-section prepared by Hess [11] has been used. The result of the computation is shown in figures 3a and 3b for winter and summer, respectively. A marked difference compared to earlier results is that the mean atmosphere is stable at almost all latitudes. The only exception worth mentioning seems to be north of 60° N. in summer, when the mean atmosphere seems to be a little unstable.

Another measure of the degree of instability which is present in the model is the time it takes to double the

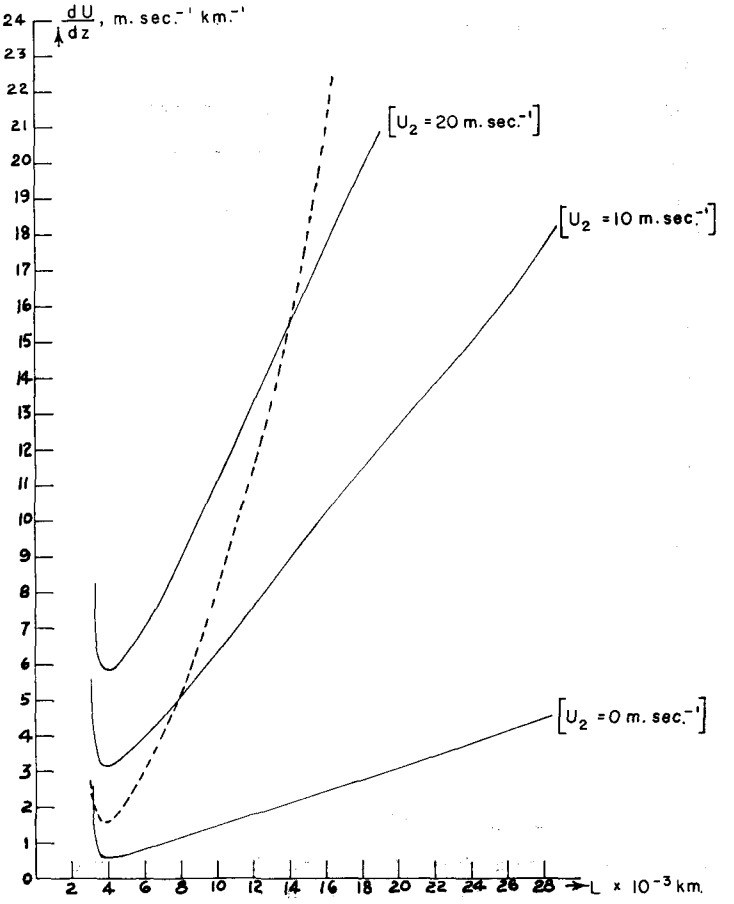

FIGURE 2.—Diagram giving the division between stable and unstable regions for different values of the zonal velocity, U_2. The dashed line is the corresponding curve for a model with vanishing mean divergence. The horizontal axis gives wavelength in thousands of km., the vertical axis vertical wind shear in the unit m. sec.$^{-1}$ km.$^{-1}$.

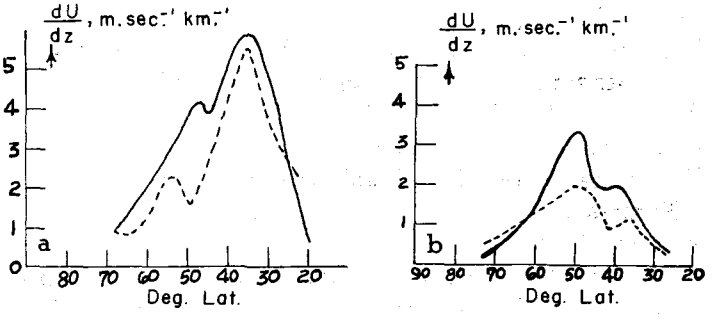

FIGURE 3.—The dashed curves give the averaged vertical wind shear in the layer between 800 and 400 mb. in the unit m. sec.$^{-1}$ km.$^{-1}$ as a function of latitude obtained from Hess' [11] cross-section. The solid curves give the critical wind shear corresponding to the zonal wind as taken from the cross-section at 600 mb. (a) Winter, (b) Summer.

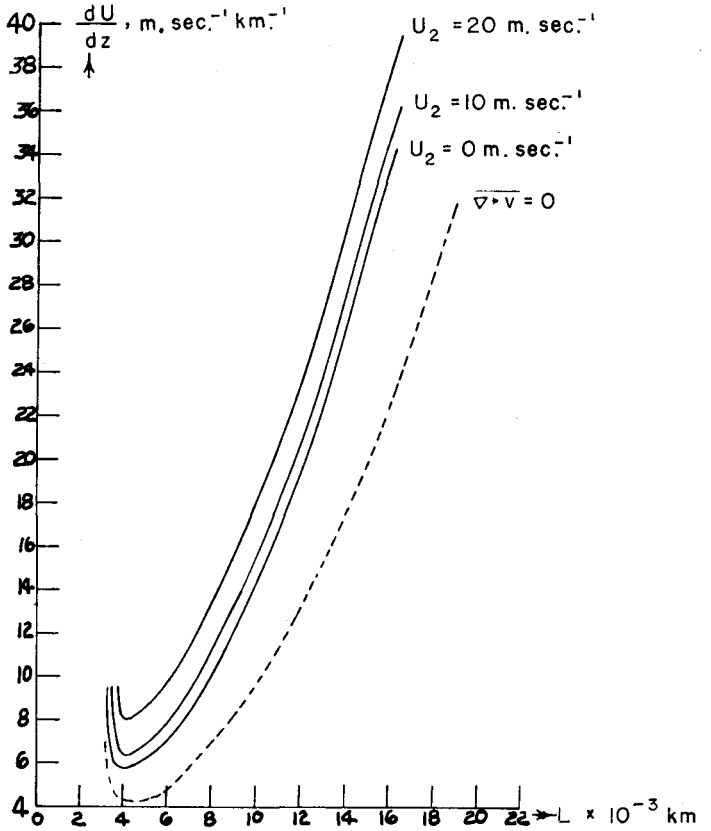

FIGURE 4.—Diagram showing the vertical wind shear necessary to double the amplitude of a wave in 24 hours as a function of wavelength for different values of the zonal velocity U_2. The dashed curve gives the same for the model with vanishing mean divergence.

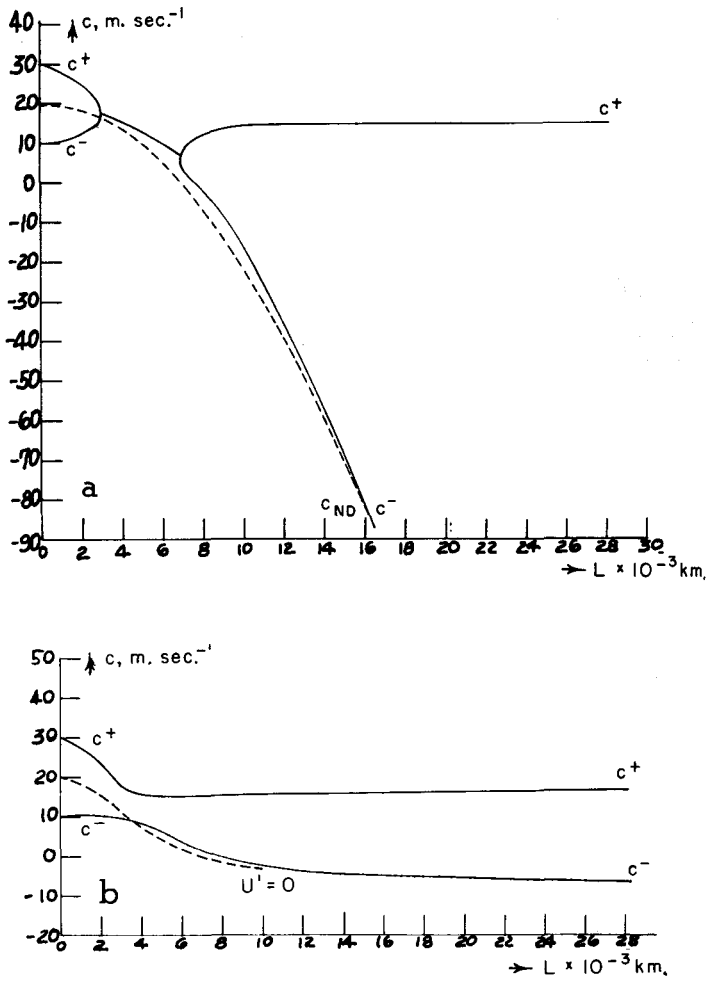

FIGURE 5.—(a) Phase-velocity as function of wavelength for the model without mean divergence, (b) the corresponding figure for a model with mean divergence. The dashed line in (a) is the Rossby speed, while the dashed curve in (b) corresponds to $U'=0$ (no vertical wind shear). Parameters: $U_2=20$ m. sec.$^{-1}$, $dU/dz=4$ m. sec.$^{-1}$ km.$^{-1}$.

amplitude of a certain perturbation. This time will of course also depend on the wind speed U_2 in the model with mean divergence. Figure 4 contains curves giving the vertical wind shear necessary to double the amplitude in 24 hours as a function of wavelength for different values of U_2 in the model with mean divergence. The curve corresponding to the same condition for the model with vanishing mean divergence is plotted for comparison. This figure illustrates even more clearly than figure 2, the decreased instability caused by the mean divergence. As an example taken from figure 4 it may be mentioned that for $L=4000$ km. and $U_2=20$ m. sec.$^{-1}$ a vertical wind shear almost twice as large as in the model without mean divergence is needed to double the amplitude in one day.

Figures 5–8 give the phase speed c as a function of wavelength in the two models for different combinations of U_2 and U'. The curves in figures 5a–8a were computed from (6.3) with $r=0$, corresponding to no mean divergence, and in the figures 5b–8b with $r\neq 0$. The main feature in these figures is of course the great difference between the curves c^- (corresponding to the negative sign in front of the square root), assuring us that no excessive retrogression takes place in the modified model. Figure 5 illustrates a case where the modified model is stable for all wavelengths, while the model without mean divergence actually is unstable in a band from about 3100 km. to about 7000 km. Note also in figure 6 that the modified model is unstable in a shorter interval than the non-modified. This is, however, not invariably so. When the zonal speed U_2 is small and dU/dz is large the modified model will be unstable in a broader band of wavelength. This fact is illustrated in figures 7a and 7b, corresponding to $U_2=10$ m. sec.$^{-1}$ and $dU/dz=8$ m. sec.$^{-1}$ km.$^{-1}$. Figures 8a and 8b finally illustrate a case where $U_2=10$ m. sec.$^{-1}$ and $dU/dz=4$ m. sec.$^{-1}$ km.$^{-1}$. In these diagrams the band of unstable waves is about the same.

Figures 5a–8a contain for comparison the speed of waves in a non-divergent, barotropic atmosphere, the Rossby speed, while figures 5b–8b contain the wave speed corresponding to $dU/dz=0$. For large values of the wavelength the speed for dU/dz 0 and $dU/dz=0$ are

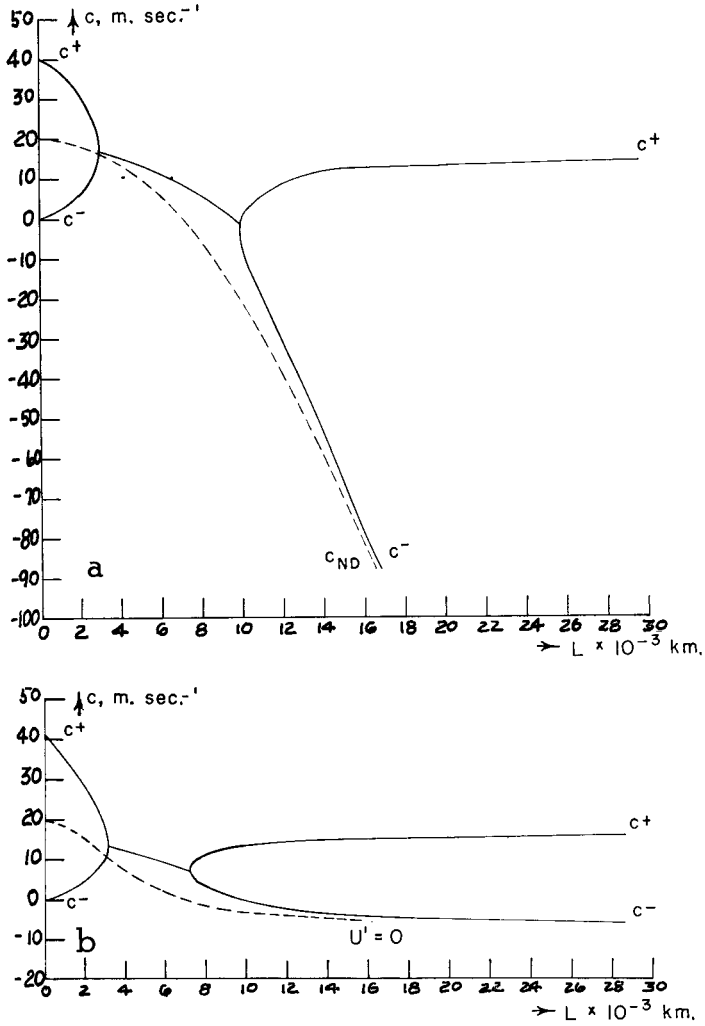

FIGURE 6.—Same as figure 5, but with parameters: U_2=20 m. sec.$^{-1}$, dU/dz=8 m. sec.$^{-1}$ km.$^{-1}$.

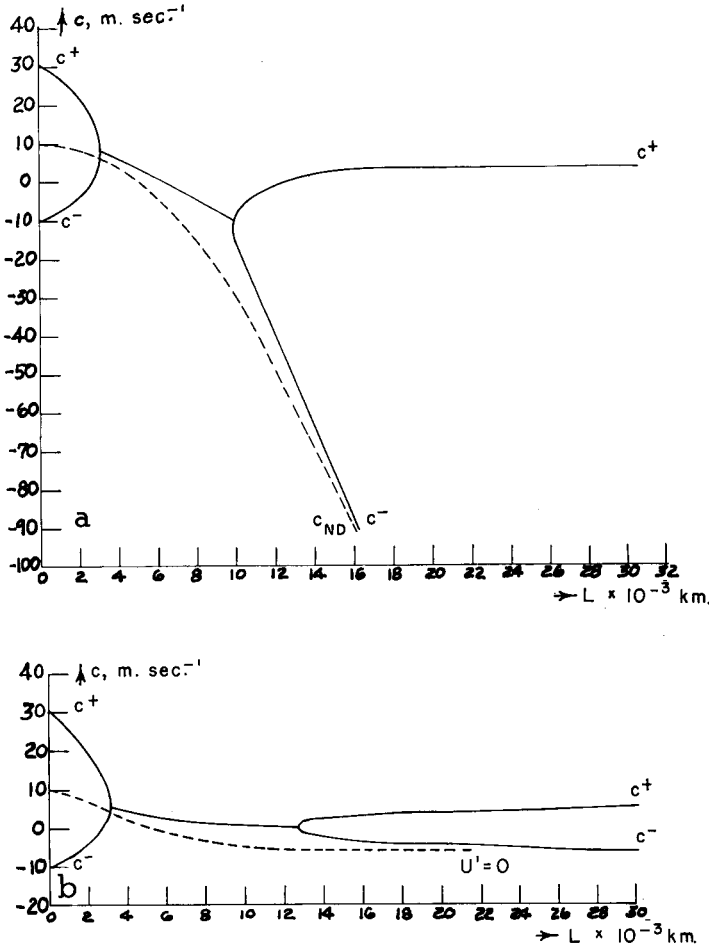

FIGURE 7.—Same as figure 5, but with parameters: U_2=10 m. sec.$^{-1}$, dU/dz=8 m. sec.$^{-1}$ km.$^{-1}$.

about the same, while the speed of the waves in a baroclinic atmosphere is somewhat larger than in an atmosphere with no vertical wind shear.

7. ON THE VERTICAL VARIATION OF STATIC STABILITY

The evaluation of divergence in sections 2 and 5 depends to a large extent on the vertical variation of static stability. We have in the earlier sections used a variation described by (2.8), where the static stability varies inversely to the square of pressure.

The tropospheric part of a mean atmosphere is usually characterized by a certain lapse-rate, $\gamma=-\partial T/\partial z$. The most straightforward way to compute the static stability $\sigma=-\alpha\partial\ln\theta/\partial p$ as it appears in models for numerical integration would therefore be to assume a certain value for γ and then compute the variation of σ. It is, however, of great convenience in many problems to have σ as a rather simple function of pressure. In this section we shall show that a formula of the form (2.8) will describe the vertical variation of temperature in the atmosphere to a good approximation. Let us write (2.8) in the form:

$$\sigma=\frac{a}{p^2} \tag{7.1}$$

where a is a constant determined in such a way that σ at some pressure level, for instance 600 mb., is equal to a standard value determined from a mean atmosphere. Let us next try to find $T=T(p)$ corresponding to (7.1) by writing

$$\sigma=-\alpha\frac{\partial\ln\theta}{\partial p}=\frac{R}{p}\left(\frac{R}{c_p}\frac{T}{p}-\frac{dT}{dp}\right) \tag{7.2}$$

we find that the temperature has to satisfy the following differential equation of the Euler type

$$p\frac{dT}{dp}-\frac{R}{c_p}T+\frac{a}{R}=0. \tag{7.3}$$

The solution to (7.3) is

$$T=T(p)=\frac{a}{R^2c_p}+Cp^{\frac{R}{c_p}}. \tag{7.4}$$

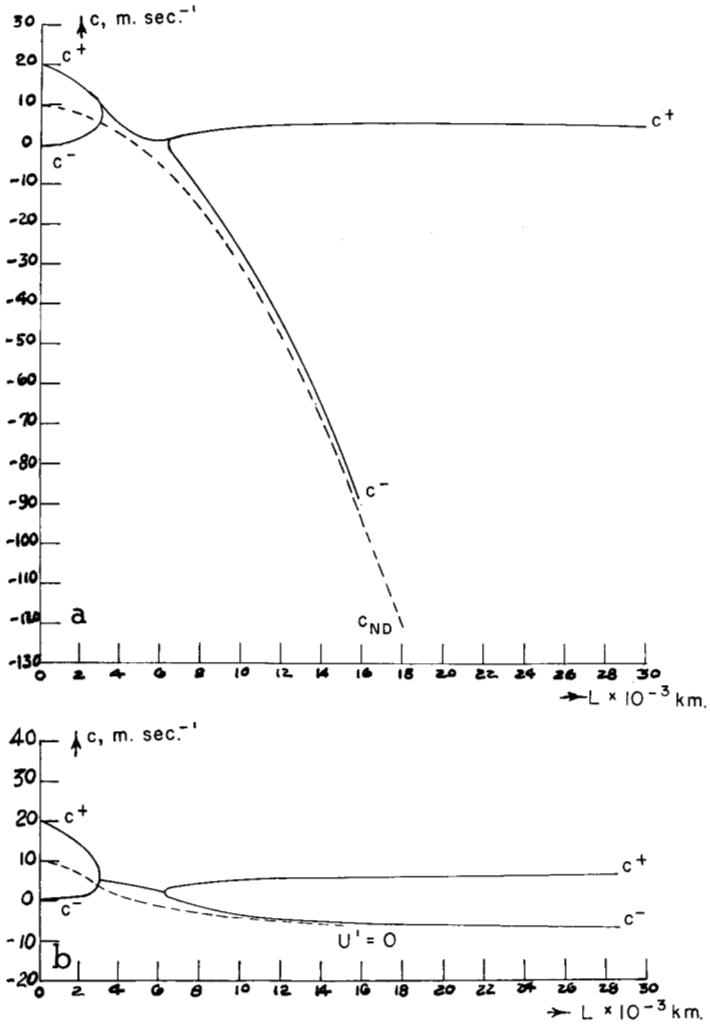

FIGURE 8.—Same as figure 5, but with parameters: $U_2=10$ m. sec.$^{-1}$, $dU/dz=4$ m. sec.$^{-1}$ km.$^{-1}$.

The arbitrary constant C can be determined by fixing the temperature at a certain pressure, say, 600 mb. We obtain then

$$T=T(p)=\frac{a}{R^2}c_p+\left(T_2-\frac{a}{R^2}c_p\right)\left(\frac{p}{p_2}\right)^{\frac{R}{c_p}}. \qquad (7.5)$$

The temperature distribution given by (7.5) is plotted in figure 9 as the full curve. The dashed curve gives the temperature distribution in the standard atmosphere, while the dotted curve is taken from Defant and Taba [7] corresponding to the air mass between the polar-front jet and the subtropical jet. It is seen that the three curves follow each other quite closely, and we may therefore conclude that the assumption (2.8) represents mean conditions in the troposphere in the westerlies quite well.

For use in the next section we shall need the temperature distribution in the stratosphere. For simplicity we shall assume that the stratosphere is isothermal with a temperature corresponding to the one obtained from (7.5)

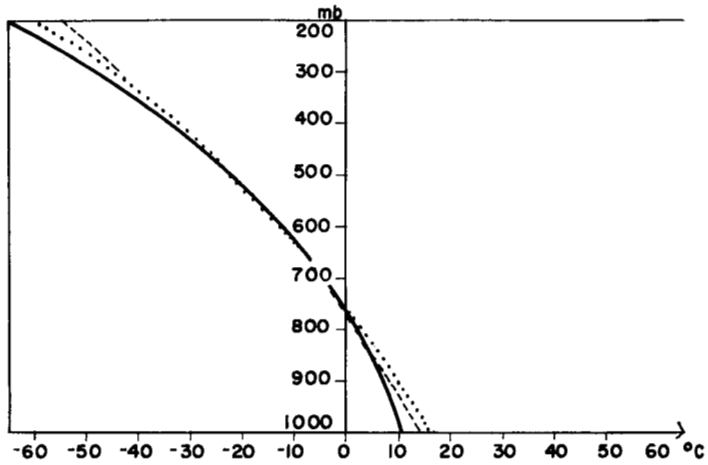

FIGURE 9.—Temperature as a function of pressure corresponding to a variation of static stability inversely proportional to the square of pressure (solid curve). The dashed curve gives temperature as function of pressure in the standard atmosphere, while the dotted curve is the temperature as function of pressure in the air mass between the polar jet and the subtropical jet as given by Defant and Taba [7].

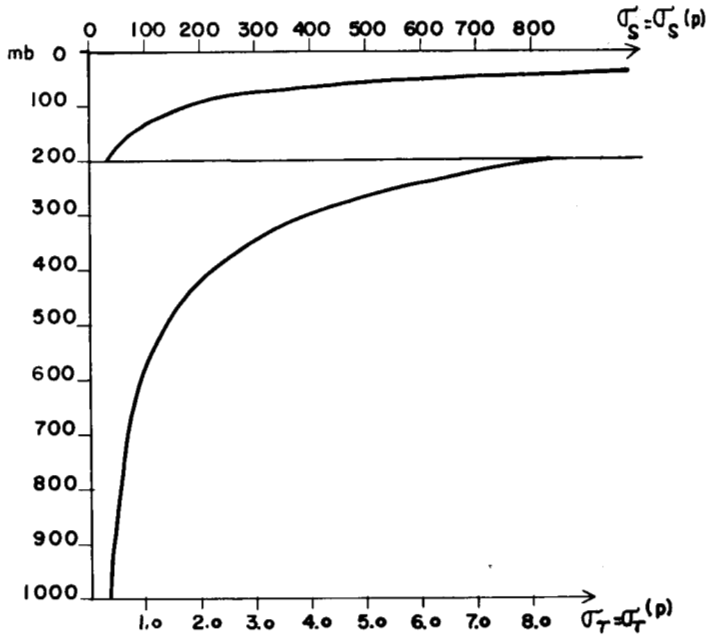

FIGURE 10.—Static stability as a function of pressure in troposphere and stratosphere, when the stability is inversely proportional to the square of pressure.

for $p=p_0=200$ mb. The stability will then vary in the following way:

$$\sigma_S=\frac{R^2T_S}{c_p}\frac{1}{p^2}=\frac{b}{p^2}. \qquad (7.6)$$

The stability profile as determined from (7.1) and (7.6) is shown in figure 10. It is seen that the static stability varies greatly in troposphere and stratosphere and further that the tropopause is characterized by a jump in stability.

8. SOME EXAMPLES OF VERTICAL PROFILES OF THE VERTICAL VELOCITY

In section 5 we neglected the vertical velocity at 200 mb. in comparison with that at 600 mb. As the 200-mb. surface usually in the westerlies is in the stratosphere one can from many considerations justify this neglect. In order actually to measure the ratio between the two quantities certain diagnostic computations of the vertical profile of ω have been performed. These computations were made with a model slightly different from the one described in this paper, because special attention was paid to the influence of the stratosphere on the vertical profile of ω. The ω-equation was obtained from the vorticity and adiabatic equations in the forms

$$\frac{\partial \zeta}{\partial t}+\mathbf{V}\cdot\nabla(\zeta+f)+\omega\frac{\partial \zeta}{\partial p}=(\zeta+f)\frac{\partial \omega}{\partial p} \tag{8.1}$$

and

$$\frac{\partial}{\partial t}\left(\frac{\partial \psi}{\partial p}\right)+\mathbf{V}\cdot\nabla\left(\frac{\partial \psi}{\partial p}\right)+\frac{\sigma}{f}\omega=0 \tag{8.2}$$

by the usual procedure. In this way we arrive at an equation for the vertical velocity in the form

$$(\nabla^2\psi+f)\frac{\partial^2\omega}{\partial p^2}+\sigma\nabla^2\omega+\frac{k}{p}\frac{\partial\nabla^2\psi}{\partial p}\omega=F(x,y,p) \tag{8.3}$$

with

$$F(x,y,p)=\frac{\partial}{\partial p}(\mathbf{V}\cdot\nabla\eta)-\nabla^2\left(\mathbf{V}\cdot\nabla\frac{\partial \psi}{\partial p}\right). \tag{8.4}$$

In the troposphere we assume that

$$\mathbf{V}=\mathbf{V}_2+A(p)\mathbf{V}', \quad \sigma=\frac{a}{p^2} \tag{8.5}$$

and in the stratosphere that

$$\mathbf{V}=B(p)\mathbf{V}_0, \quad \sigma=\frac{b}{p^2}. \tag{8.6}$$

The functions $A(p)$ and $B(p)$ were in fact determined in such a way that they are consistent with the assumption that $\nabla\sigma=0$ (see Berkofsky [1]) and further such that the wind is continuous at $p=p_0=200$ mb. (see fig. 11). When the approximations (8.5) and (8.6) are introduced in (8.3) we arrive at two equations, one for the troposphere and one for the stratosphere.

As we are here interested in the vertical variation of ω, we shall replace $\nabla^2\omega$ by $-\beta\omega$, where β is an inverse measure of horizontal scale. By doing this we restrict ourselves to a consideration of essentially one scale. β was here chosen as corresponding to the wavelength of maximum instability ($L=4000$ km.). With this restriction the two equations obtained from (8.3) reduce to ordinary differential equations in ω, which then should be solved using appropriate boundary conditions.

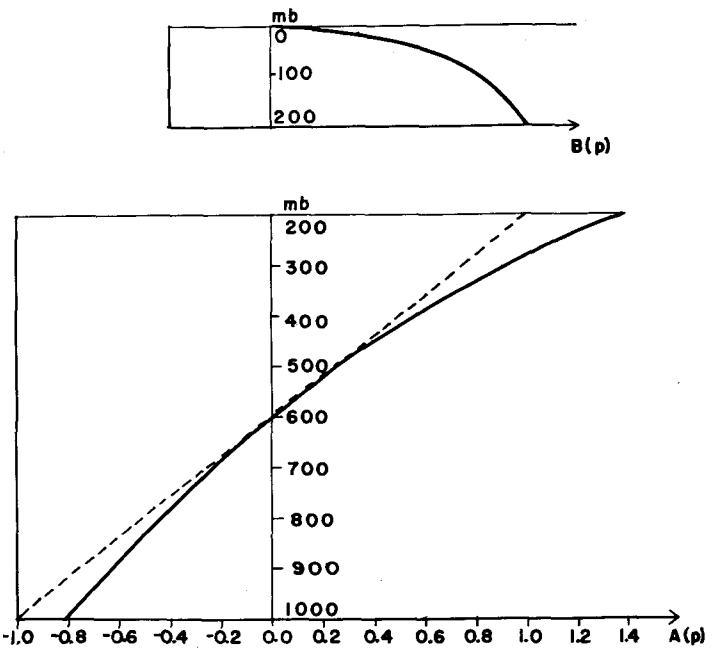

FIGURE 11.—The functions $A(p)$ and $B(p)$ characterizing the variation of the horizontal wind with pressure in the model used for diagnostic computations of vertical velocity. The dashed curve in the lower figure corresponds to the case where $A(p)$ is a linear function of pressure.

We shall use $\omega=0$ for $p=0$ and $p=p_4=1000$ mb. Furthermore, we need an internal boundary condition for $p=p_0=200$ mb., where the solution to the stratospheric equation should be matched together with the solution to the tropospheric equation. The level $p=p_0=200$ mb. represents in the present considerations the tropopause as well as the level of maximum wind. These two levels need not in all cases be the same in reality, but synoptic investigations (Defant and Taba [7]) show that they are close to each other, usually with the level of maximum wind a little lower than the tropopause. We way, therefore, at the level $p=p_0$ apply a boundary condition natural for a discontinuity surface for stability. Such boundary conditions have been treated by Lowell [12]. The vertical velocity should be continuous at the tropopause and further should $(\partial\omega/\partial p)_S\simeq(\partial\omega/\partial p)_T$ which means that the first derivative in the p-direction should be continuous. These two conditions have therefore been applied at $p=p_0$.

The solution to the two equations obtained from (8.3), with the boundary conditions mentioned above, is quite laborious. For the general case it has not been possible to find analytical solutions. A numerical integration of the two equations has therefore been performed. The method used in the numerical solutions has been the Runge-Kutta method, which is most convenient in cases of internal boundary conditions. Examples of solutions are presented in figures 12 and 13. In these cases the stream functions at 600 mb. and for the thermal flow

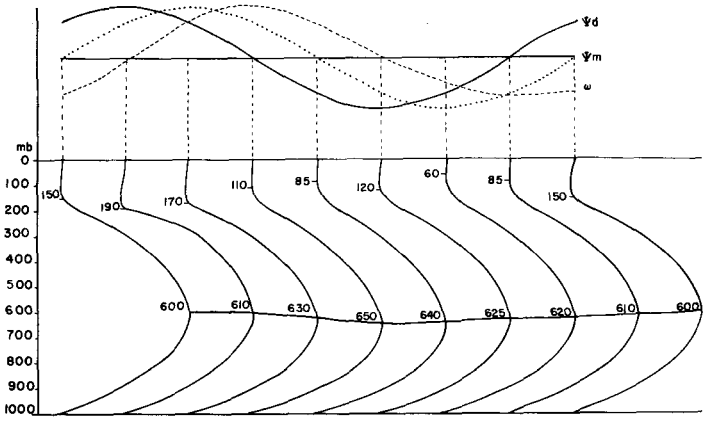

FIGURE 12.—The vertical velocity as a function of pressure in different points of a baroclinic wave, where the thermal stream function is lagging ⅛ of a wavelength behind the stream function at 600 mb. (see upper part of the figure). The dashed curve in the upper part of the figure gives the vertical velocity through the baroclinic wave at 600 mb.

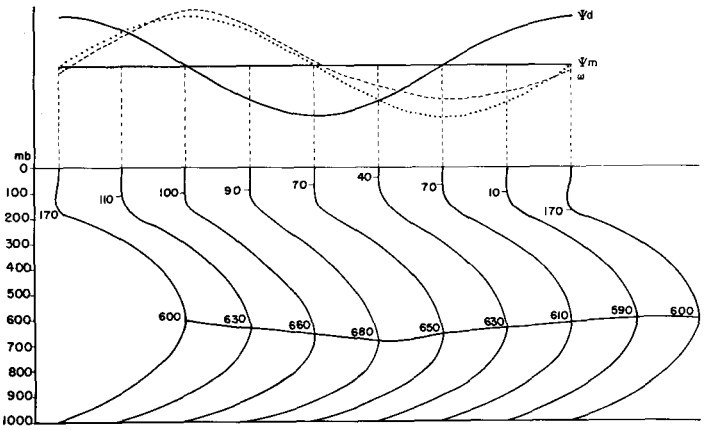

FIGURE 13.—Same as figure 12, but with phase-difference of ¼ of a wavelength between the thermal stream function and the stream function at 600 mb.

between 800 and 400 mb. were specified as simple sinusoidal waves having a certain phase difference. Figure 12 corresponds to the case where the thermal field is lagging ⅛ of the wavelength behind the field at 600 mb., while figure 13 has a phase difference of ¼ of a wavelength. All constants were computed for eight different points. The computation gave then the eight vertical profiles represented in the figures, which in the upper part contain a schematic picture of the temperature and pressure wave and also the horizontal profile through the baroclinic wave of the vertical velocity at 600 mb. On each of the profiles is given the level of maximum vertical velocity and the levels where ω has a zero point different from those at the boundaries. It should further be mentioned that each profile is normalized in such a way that the maximum value is unity.

Of importance for the discussion in the preceding sections are the following features:

(a) A zero point for the vertical velocity appears somewhat higher than the level of maximum horizontal wind. The pressures of the zero points vary systematically through the wave, and we may state that the values of ω obtained above the zero point are extremely small.

(b) ω_0 at 200 mb. is not exactly zero, but it is true that $\omega_0 \ll \omega_2$ where ω_2 is at 600 mb. This characteristic justifies the approximation made in section 5.

(c) The non-divergent level varies systematically through the baroclinic wave with the result that this level does not coincide with a pressure level.

(d) It is a limitation in the present calculation that the tropopause level has been assumed at a constant pressure (200 mb.). In reality we may therefore expect a larger variation of the level of nondivergence.

9. SUMMARY AND CONCLUSIONS

Sections 2–4 contain a derivation and discussion of the prognostic equation for the 500-mb. flow where attention is focused on the term which controls the ultra-long waves. It is shown that the numerical value of the coefficient is related to the vertical variation of the horizontal wind and the corresponding variation of the static stability. The numerical value determined in this way agrees well with the one obtained empirically by Cressman [6] and Bolin [2].

Section 5 generalizes the results obtained in sections 2–4 to a simple two-parameter model. It is shown that the simplest way to control the ultra-long waves in a baroclinic model is to introduce a mean divergence in the troposphere. The mean divergence may in the first approximation be estimated barotropically corresponding to the well-known fact that the mean motion in the atmosphere is almost barotropic.

The influence of an existing mean divergence in the atmospheric layer under consideration on the baroclinic instability is investigated in section 6. The main result is that the mean divergence stabilizes the shorter waves to some extent, beside the effect of decreasing the retrogression of the ultra-long waves considerably. An application of the stability criteria derived in this section to a mean cross-section for the atmosphere shows that the mean atmosphere is baroclinically stable at almost all latitudes.

A justification of certain approximate relations used in the earlier sections is given in sections 7 and 8 of which the former is concerned with the vertical variation of the static stability, while the latter gives certain diagnostic results of computations of vertical profiles of the vertical velocity.

Any model designed for numerical prediction of tropospheric flow pattern must contain an effect which at least expresses the quasi-stationary behavior of the ultra-long waves. According to results obtained by Burger [3] we

cannot expect to express more than this as long as we use the vorticity equation as the prognostic equation. One possible way of controlling the ultra-long waves is demonstrated in this paper, where we have made use of the observed barotropic character of these waves. Certain modifications of the behavior of shorter waves is also obtained by this procedure. It is quite likely that a more sophisticated introduction of the mean divergence, which seems to be the important quantity, into a tropospheric model may change the behavior of the Rossby type of waves still more.

ACKNOWLEDGMENTS

The author would like to thank Dr. G. P. Cressman and Dr. F. G. Shuman for a number of interesting discussions on the subject treated in this paper.

REFERENCES

1. L. Berkofsky, "A Three-Parameter Baroclinic Numerical-Prediction Model," *Journal of Meteorology*, vol. 13, No. 1, Feb. 1956, pp. 102–111.
2. B. Bolin, "An Improved Barotropic Model and Some Aspects of Using the Balance Equation for Three-Dimensional Flow," *Tellus*, vol. 8, No. 1, Feb. 1956, pp. 61–75.
3. A. P. Burger, "Scale Consideration of Planetary Motions of the Atmosphere," *Tellus*, vol. 10, No. 2, May 1958, pp. 195–205.
4. J. G. Charney, "The Dynamics of Long Waves in a Baroclinic Westerly Current," *Journal of Meteorology*, vol. 4, No. 5, Oct. 1947, pp. 135–162.
5. J. G. Charney, "On a Physical Basis for Numerical Prediction of Large-Scale Motions in the Atmosphere," *Journal of Meteorology*, vol. 6, No. 6, Dec. 1949, pp. 371–385.
6. G. P. Cressman, "Barotropic Divergence and Very Long Atmospheric Waves," *Monthly Weather Review*, vol. 86, No. 8, Aug. 1958, pp. 293–297.
7. F. Defant and H. Taba, "The Break Down of Zonal Circulation During the Period January 8 to 13, 1956, the Characteristics of Temperature Field and Tropopause and its Relation to the Atmospheric Field of Motion," *Tellus*, vol. 10, No. 4, Nov. 1958, pp. 430–450.
8. E. T. Eady, "Long Waves and Cyclone Waves," *Tellus*, vol. 1, No. 3, Aug. 1949, pp. 33–52.
9. A. Eliassen, "Simplified Dynamic Models of the Atmosphere, Designed for the Purpose of Numerical Weather Prediction," *Tellus*, vol. 4, No. 3, Aug. 1952, pp. 145–156.
10. E. Eliasen, "A Study of the Long Atmospheric Waves on the Basis of Zonal Harmonic Analysis," *Tellus*, vol. 10, No. 2, May 1958, pp. 206–216.
11. S. L. Hess, "Some New Mean Meridional Cross Sections Through the Atmosphere," *Journal of Meteorology*, vol. 5, No. 6, Dec. 1948, pp. 293–300.
12. S. C. Lowell, "The Boundary Conditions at the Tropopause," *Tellus*, vol. 3, No. 2, May 1951, pp. 78–81.
13. N. A. Phillips, "A Simple Three-Dimensional Model for the Study of Large-Scale Extratropical Flow Patterns," *Journal of Meteorology*, vol. 8, No. 6, Dec. 1951, pp. 381–394.
14. N. A. Phillips, "Energy Transformations and Meridional Circulations Associated with Simple Baroclinic Waves in a Two-Level, Quasi-Geostrophic Model," *Tellus*, vol. 6, No. 3, Aug. 1954, pp. 273–286.
15. N. A. Phillips, "Geostrophic Errors in Predicting the Appalachian Storm of November 1950," *Geophysica*, vol. 6, No. 3–4, 1958, pp. 389–405.
16. P. D. Thompson, "On the Theory of Large-Scale Disturbances in a Two-Dimensional Baroclinic Equivalent of the Atmosphere," *Quarterly Journal of the Royal Meteorological Society*, vol. 79, No. 339, Jan. 1953, pp. 51–69.
17. A. Wiin-Nielsen, "On Certain Integral Constraints for the Time-Integration of Baroclinic Models," *Tellus*, vol. 11, No. 1, Feb. 1959, pp. 45–59.
18. P. M. Wolff, "The Error in Numerical Forecasts Due to Retrogression of Ultra-Long Waves," *Monthly Weather Review*, vol. 86, No. 7, July 1958, pp. 245–250.

511937—59——4